revista principia 30 anos
Revelando e explicando o futuro
ISSN 2447-9187

https://doi.org/10.18265/2447-9187a2026id9249

ORIGINAL ARTICLE

SUBMITTED October 6, 2025
APPROVED April 24, 2026
PUBLISHED ONLINE July 3, 2026
FINAL FORMATTED VERSION 03/09/2026
ASSOCIATE EDITOR
Profa. Dra. Natalia de Souza Correia

Impact of permeable concrete pavement clogging and subgrade soil type on peak urban flood flow reduction in Fortaleza, Brazil

Francisco de Assis Cavalcanti Bezerra [1]
Karina de Lima [2]
Larissa Virgínia da Silva Ribas [3]
Wellington Lorran Gaia Ferreira [4] *
Verônica Teixeira Franco Castelo Branco [5]

[1] assisbezerradrenagem@yahoo.com.br
[2] karina.lima@det.ufc.br
[5] veronica@det.ufc.br
Universidade Federal do Ceará (UFC), Fortaleza, Ceará, Brazil

[3] larissa.ribas@det.ufc.br
Universidade Federal da Bahia (UFBA), Salvador, Bahia, Brazil

[4] wellington.ferreira@ufersa.edu.br
Universidade Federal Rural do Semi-Árido (UFERSA), Caraúbas, Rio Grande do Norte, Brazil

* *Corresponding author.*

ABSTRACT: This study aimed to evaluate the effect of applying permeable pavements under different clogging conditions and foundation soil types on reducing peak urban flood flows. Twelve concrete slabs were analyzed, six with and six without an internal geotextile membrane, to assess the effectiveness of cleaning. Infiltration tests revealed that, even after cleaning, the permeability did not return to its original condition, and the inclusion of the geotextile membrane did not demonstrate a positive impact on permeability recovery. These findings highlight the need for more effective maintenance strategies. The application of permeable pavements was simulated by modeling a sub-basin in the city of Fortaleza, Ceará. The effects on the flood peak were considered across different types of foundation soils, such as clayey and sandy soils. Furthermore, spatial analysis of 300 infiltration tests enabled the identification of priority areas for permeable pavement implementation across the city. The modeling results indicated a reduction of up to 20.83% in peak flows with the implementation of permeable pavements, reinforcing the potential of this technology in sustainable stormwater management and flood control. This approach can be a viable solution for managing urban runoff in similar tropical regions and preventing widespread flooding.

Keywords: clogging; flooding; hydrological modeling; permeable concrete; urban drainage.

Impacto da colmatação de pavimentos de concreto permeáveis e do tipo de solo de fundação na redução do pico de cheia urbana em Fortaleza, Brasil

RESUMO: *Este estudo teve como objetivo avaliar o efeito da aplicação de pavimentos permeáveis sob diferentes condições de colmatação e tipos de* *solo de fundação na redução de picos de cheia urbana. Doze placas de concreto foram analisadas, seis com membrana geotêxtil interna e seis sem esse tipo de membrana, para avaliar a eficácia da limpeza. Os ensaios de infiltração mostraram que, mesmo após a limpeza, a permeabilidade não retornou à sua condição original, e a inclusão da membrana geotêxtil não demonstrou impacto positivo na recuperação da permeabilidade. Esses achados ressaltam a necessidade de estratégias de manutenção mais eficazes. A aplicação de pavimentos permeáveis foi simulada por meio da modelagem de uma sub-bacia na cidade de Fortaleza, Ceará. Os efeitos no pico de inundação foram considerados em diferentes tipos de solos de fundação, como solos argilosos e arenosos. Além disso, uma análise de 300 ensaios de infiltração permitiu identificar as áreas mais adequadas para a implementação de pavimentos permeáveis em Fortaleza. Os resultados indicaram uma redução de até 20,83% nos picos de vazão com a implementação de pavimentos permeáveis, reforçando o potencial dessa tecnologia na gestão sustentável de águas pluviais e no controle de inundações. Essa abordagem pode ser uma solução viável para o gerenciamento do escoamento urbano em regiões tropicais semelhantes e para a prevenção de inundações generalizadas.*

Palavras-chave: *alagamentos; colmatação; concreto permeável; drenagem urbana; modelagem hidráulica.*

1 Introduction

The urbanization process leads to an increase in soil impermeabilization, as urban infrastructure is predominantly composed of impervious surfaces such as asphalt, concrete, and buildings, which significantly hinder natural stormwater infiltration. Recent studies indicate that, globally, urban areas have expanded rapidly, with impervious surface coverage increasing substantially over recent decades, directly intensifying surface runoff and flood risks (Liu *et al*., 2012; Zhou *et al*., 2015). In Brazil, this challenge is particularly acute in fast-growing cities, where unplanned urban expansion and the reduction of green areas constrain infiltration capacity and overload drainage systems. This issue is even more pronounced in tropical regions, such as Fortaleza, Ceará (CE), Brazil, where high-intensity and short-duration rainfall events exacerbate peak runoff generation. As a result, the reduction of permeable surfaces contributes to increased surface runoff volumes and velocities, favoring the occurrence of urban flooding and related socio-environmental impacts (Du *et al*., 2015; Lima *et al*., 2025; Taleghani, 2018; Wang *et al*., 2018). Indeed, as highlighted by Teixeira and Meneses Filho (2020), the reduction of permeable areas in urban environments directly alters the hydrological response of watersheds, increasing runoff and intensifying flooding problems.

According to Marinho *et al*. (2020) and Batezini *et al*. (2021), permeable pavement is an alternative to reduce the negative impacts of increased surface runoff resulting from intense urbanization. These systems can be classified into different types, including permeable asphalt, pervious (porous) concrete, and permeable interlocking concrete block pavements (PICP), each with distinct structural and hydraulic characteristics. Among these, pervious concrete is characterized by a highly interconnected pore structure that allows water to infiltrate through the material, promoting temporary storage and subsequent percolation into into the subgrade or internal drainage layers.

This behavior aligns with its application as Low Impact Development (LID) strategy for sustainable urban drainage (Ahiablame; Engel; Chaubey, 2012; Li; Kayhanian; Harvey, 2013). The infiltration process depends on the hydraulic properties of both the pavement and the subgrade, enabling reductions in surface runoff and peak flow. In the case of the coastal basins of Fortaleza, hydrological modeling studies demonstrates that rainfall events significantly increase pollutant loads and highlight the importance of efficient urban drainage management strategies (Mesquita; Pereira; Lima Neto, 2020).

Despite the advantages associated with using permeable pavement, the primary challenge is the clogging process. Clogging can be technically defined as the progressive reduction of pore connectivity and hydraulic conductivity caused by the accumulation and retention of fine particles within the void structure of the material. This process occurs when sediments transported by runoff or atmospheric deposition infiltrate and become trapped in the pores, leading to a decline in infiltration capacity (Wang *et al*., 2018). According to Oliveira (2017), clogging is a complex phenomenon influenced by multiple factors, including pore structure, sediment granulometry, rainfall intensity, and event duration. It typically develops over months to years of operation, depending on environmental exposure and maintenance conditions. Different types of clogging can be identified, such as surface clogging (accumulation at the top layer), internal clogging (particle retention within the pore network), and structural clogging (changes in the material matrix). This study focuses primarily on internal clogging, as it directly affects the permeability of the concrete matrix. As clogging progresses, permeable pavements experience a gradual loss of hydraulic performance, ultimately reducing their effectiveness in stormwater management (Kia; Wong; Cheeseman, 2017). The physical mechanisms governing clogging, including sediment transport, filtration, and particle retention within porous media, have been widely discussed in the literature, reinforcing the importance of understanding this phenomenon for the long-term performance of permeable systems (Brown; Borst, 2014; Lucke; Beecham, 2011).

Sansalone *et al*. (2012) reports that the effectiveness of maintenance on permeable concrete pavements depends on the location and particle size of the clogging materials. Commonly deployed remediation techniques include vacuum sweeping, for the removal of surface debris, and pressure washing, which is effective for unclogging pores where sediments have already begun to penetrate. Larger particles tend to remain closer to the surface, facilitating cleaning, whereas finer particles require methods that combine pressure and reverse flow (Kia; Wong; Cheeseman, 2017; Sandoval *et al*., 2022). In this study, the maintenance process was simulated via pressure washing, a technique that proves critical for restoring minimum residual permeability and preventing the progression of deep clogging (Radfar; Rockaway, 2016). Recent literature emphasizes that both the frequency and type of maintenance should be adapted to the rainfall regime and local sediment load to ensure the functionality of the infrastructure (Seifeddine; Amziane; Toussaint, 2023). Another important factor is the type of soil on which the pavement will be implemented. The characteristics of this substrate impact the reduction of surface runoff. Verma *et al*. (2020) affirm that various aspects can influence the soil's infiltration capacity and the transformation of rainfall into surface runoff. Selecting locations that favor infiltration for the application of permeable pavements can enhance the beneficial effects of this alternative. The Brazilian National Water Agency (ANA, 2018) presents a hydrological classification of soils, classifying them into four groups according to their runoff potential and infiltration capacity, based on the Soil Conservation Service (SCS) method (SCS, 1975). Hawkins, Theurer and Rezaeianzadeh (2019) report that some relevant aspects are not considered in this methodology and that there are watersheds with particularities underrepresented by this model. Miguel and Rennó (2020) found that using the SCS method (SCS, 1975) in some situations led to inaccurate estimates of effective precipitation. Considering this, Sartori (2004) presented other hydrological classifications for soils developed in Brazil to mitigate problems related to the use of models from other regions. However, the model suggested by SCS (1975) remains the most widely applied approach in contemporary hydrological modeling.

Therefore, the definition of the location where the permeable pavement will be implemented and the assurance of minimum permeability of the covering are essential aspects for the functionality of this solution. This study aims to evaluate the performance of permeable concrete pavements as a strategy for urban flood mitigation by integrating experimental, material, and hydrological approaches. Specifically, it seeks to: (i) assess the permeability of concrete slabs under different clogging conditions, (ii) analyze the effects of clogging on infiltration capacity over time, and (iii) simulate the impacts of permeable pavements on surface runoff and peak flow reduction. The hydrological response was modeled using the Soil Conservation Service (SCS) method, combined with Curve Number (CN) analysis and Intensity-Duration-Frequency (IDF) relationships derived from long-term rainfall data, enabling the evaluation of different soil types and urban surface scenarios in Fortaleza, Ceará, Brazil.

After this brief introduction, this article is structured in materials and methods (section 2), which describes the fabrication and tomographic analysis of permeable concrete slabs, the characterization of the study area, the procedures for determining infiltration rates, the simulation of clogging processes, the modeling of peak flooding in a macro-drainage system, and the evaluation of suitable locations for permeable pavement application in Fortaleza; results and discussion (section 3), which presents the permeability analysis of the slabs, the hydrological modeling of sub-basin A6, and the spatial mapping of priority areas for implementation; conclusions (section 4), which summarizes the main findings; and finally, references.

2 Materials and methods

The methodology adopted in this study was structured into three main stages:

1) Molding and characterization of permeable concrete pavement (PCP) slabs, including performance tests and clogging simulation;
2) Characterization of the study area, with hydrological and territorial analysis of the A-6 sub-watershed in Fortaleza, Ceará, Brazil;
3) Hydrological simulations under impermeable and permeable conditions, considering different subgrade soil types.

Figure 1 summarizes the experimental procedure, visually illustrating the sequence of activities, analyses, and tools used throughout the study.

Figure 1 ▶
Methodological flowchart for the evaluation and application of pervious concrete pavement. *Source: prepared by the authors*

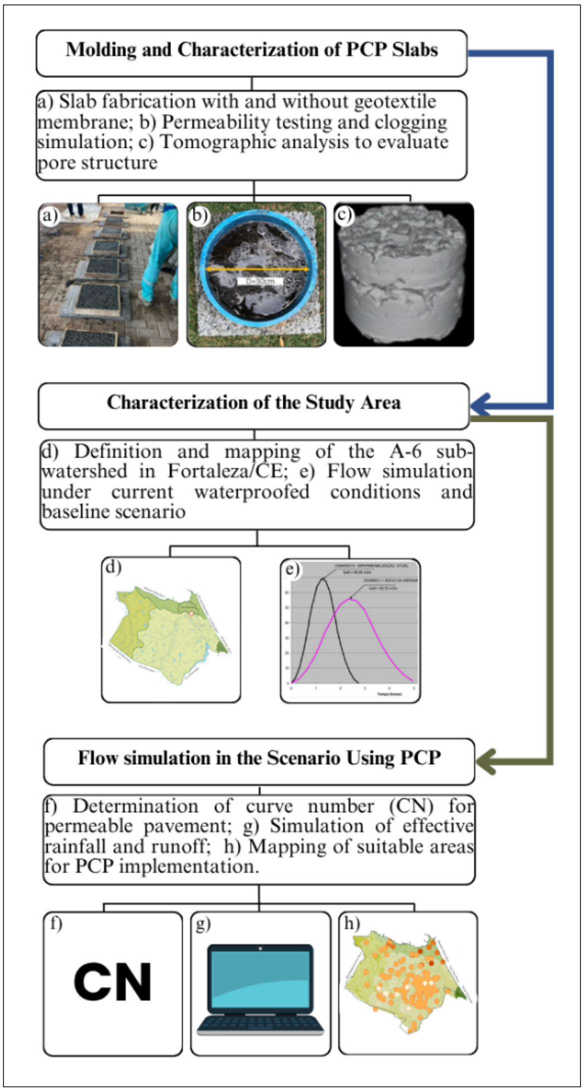

2.1 Fabrication and X-ray Computed Tomography Analysis of permeable concrete slabs

Two batches of permeable concrete slabs (Figure 2a) were produced, consisting of six specimens per batch, yielding a total of 12 samples. For each batch, three pieces were fabricated with the addition of a geotextile membrane placed at one-third of the depth of the internal structure of the slabs (Figure 2b). The geotextile membrane used in this study is a nonwoven polypropylene geotextile (Bidim type), selected for its filtration efficiency and ability to limit the penetration of fine particles into deeper layers of the concrete (Sansalone; Teng, 2004; Lucke; Beecham, 2011). The membrane has tensile strength (TS) of 7 kN/m and met the specifications of ASTM (2009). The purpose of using the geotextile membrane is to prevent deeper penetration of sediments into the slab, making it easier to restore its drainage capacity after maintenance. Although there is no standardized position for geotextile placement within pervious concrete slabs, similar approaches have been reported in studies that investigate filtration layers to control sediment transport and clogging in permeable pavement systems (Sansalone; Teng, 2004; Lucke; Beecham, 2011). All specimens were subjected to the same experimental procedures described as detailed below.

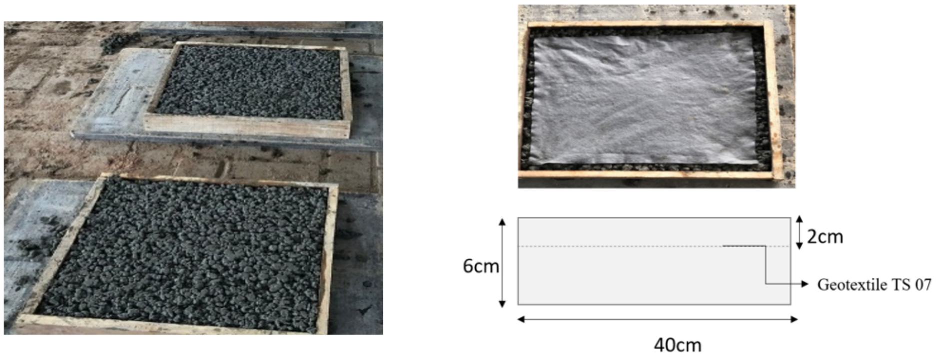

(a) (b)

Figure 2 ▶ Details of permeable concrete slabs (a), and geotextile membrane positioned at one-third of the slab depth (b). *Source: prepared by the authors*

The permeable concrete slabs were manufactured with dimensions of 40 cm × 40 cm × 6 cm. For the composition of the slabs, Apodi® CP IIF-32 cement and 0-sized aggregate were used, with a water/cement ratio of 0.31 and a cement-to-aggregate ratio of 1:2. In the absence of specific standardized procedures for molding permeable concrete slabs, the pieces were compacted manually using a wooden mallet with dimensions of 20 cm × 13 cm × 6 cm, weighing 3.03 kg and with a drop height of 20 cm. Thirteen blows were applied during compaction of each piece. It is important to highlight that the use of a vibropress (mechanical compaction) was not possible due to the need to insert the geotextile membrane. The methodology adopted in this work ensured that the slabs met the permeability and flexural strength criteria established by ABNT NBR 16416 (ABNT, 2015).

The permeability tests of the concrete slabs showed an average value greater than 7×10^{-3} m/s. The permeable concrete slabs without the geotextile membrane achieved a flexural strength of 4.27 MPa, while the slabs with the geotextile membrane reached a strength of 4.81 MPa. In both tests, the slabs met the minimum requirements established by ABNT NBR 16416 (ABNT, 2015): permeability greater than 10^{-3} m/s and flexural strength greater than 2 MPa.

To investigate the internal structure of the permeable concrete slabs, X-ray computed tomography was performed using the XT H 225 ST Nikon Metrology scanner, with a spatial resolution of 50 µm and angular velocity of 0.17°/s. The slabs were divided into two groups: with and without the geotextile membrane inserted at one-third of the height. In both cases, cylindrical specimens with 10 cm in diameter were extracted from the center of each slab using a rotary coring bit, as required by the equipment configuration (Garcia, 2022). After that, the images were reconstructed with CT Pro 3D (XT 6.10) software and processed using VGSTUDIO MAX (version 3.4.4). The tomographic analysis aimed to quantify the total pore volume, porosity percentage, and observe the degree of pore interconnectivity in three dimensions, providing qualitative and quantitative insights into the slab's permeability potential (Du Plessis *et al*., 2016).

Unlike conventional methods, which are often limited to indirect or two-dimensional measurements (e.g., porosity estimation or surface analysis), tomographic analysis allows for a more comprehensive understanding of how clogging affects the internal structure of the material. This is particularly important for this study, as the objective is to assess changes in permeability associated with internal clogging processes.

ISSN 2447-9187

2.2 Characteristics of the study area

The A-6 sub-basin region (Figure 3), with a total area of 621.06 hectares, located within the maritime drainage basin of the Municipality of Fortaleza, Ceará, was evaluated. This area was selected based on the study developed by Bezerra (2007), which estimated an increase in peak flow from 69.09 m³/s to 73.08 m³/s due to urban surface imperviousness and the implementation of a drainage system that reduces the time of concentration of the design precipitation. The region is characterized by a tropical climate (Aw, according to Köppen classification), with high temperatures throughout the year and a marked rainy season concentrated between February and May, featuring high-intensity and short-duration rainfall events. The predominant soils in the area are typically sandy and of low to moderate cohesion, generally associated with moderate to high infiltration capacity, although this behavior is significantly altered by urbanization. The sub-basin presents a high degree of urbanization, with extensive impervious coverage such as road infrastructure, buildings, and paved surfaces, which contribute to reduced infiltration, accelerated surface runoff, and escalating susceptibility to flash flooding.

Figure 3 ▼
Map of Fortaleza-CE with details of the study area (A-6 sub-watershed). *Source: prepared by the authors*

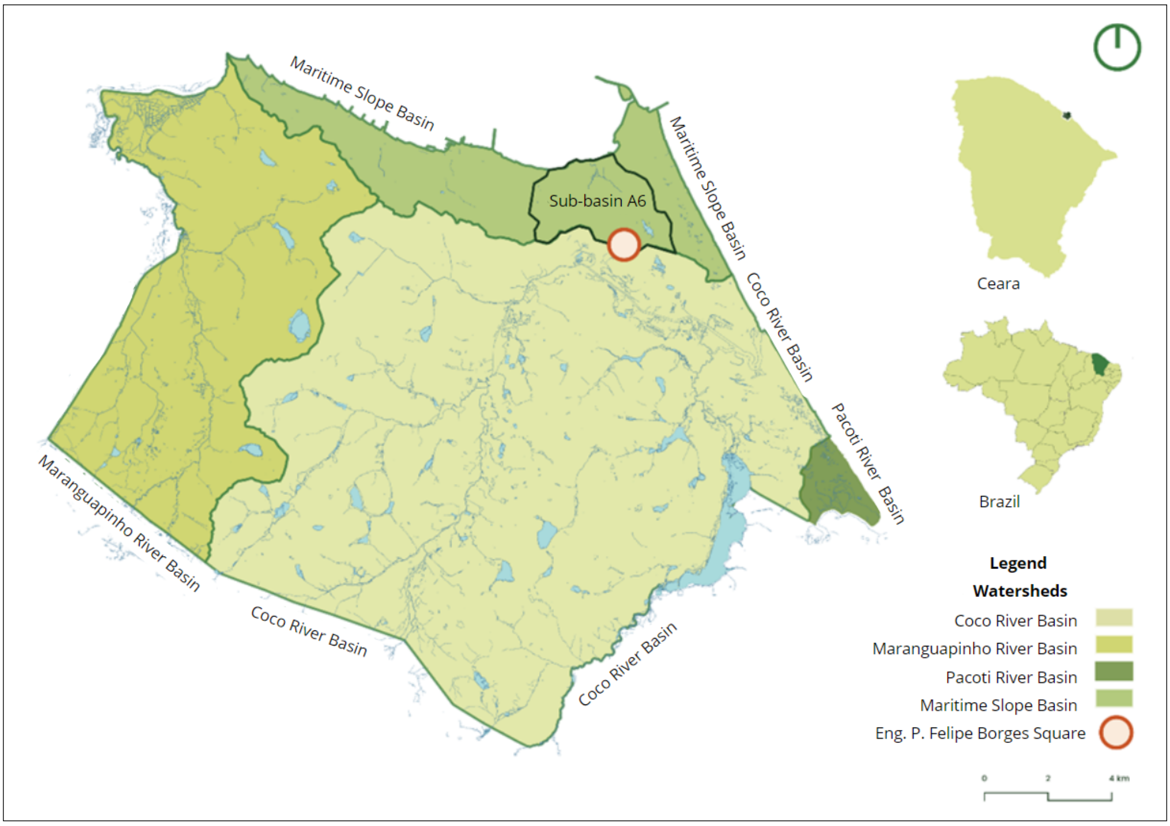

2.3 Determination of the infiltration rate

The infiltration rate of the permeable concrete slabs was determined under three conditions: (i) pristine slabs, (ii) clogged slabs, and (iii) post-maintenance slabs. The tests followed the procedures specified in ABNT NBR 16416 (ABNT, 2015). For each permeable concrete slab, a PVC ring with a diameter of 30 cm and a height of 10 cm was positioned on the surface and sealed using putty to prevent water leakage at the interface between the ring and the slab. A predefined volume of water, as specified by the standards, was then poured into the ring in a controlled manner to reach the required water head. To ensure accurate control of the water level during the test, reference markings at 5 mm and 10 mm were indicated on the inner surface of the PVC ring. The infiltration time was recorded using a digital timer, and the tests were conducted under controlled laboratory conditions to minimize external interferences, ensuring consistency across all samples and scenarios.

2.4 Clogging process simulation

To simulate the clogging process, clogging sediments were collected by sweeping the material from sidewalks and gutters around the Engineer Pedro Felipe Borges Square, located in the city of Fortaleza-CE and within the A-6 sub-watershed. The collected material, a mixture of clay, fine sand, and leaves, was deposited on the surface of the permeable concrete slabs inside a 30 cm diameter tube (Figure 4a). The clogging material presented a well-graded particle size distribution, as shown by the particle size curve (Table 1). The material exhibited a maximum particle diameter of 12.7 mm and a percentage of fines passing sieve No. 200 ranging between 10% and 20%. The use of well-graded material is particularly relevant for simulating clogging, as larger particles tend to fill surface pores, while finer particles penetrate deeper into the pore structure, promoting a more representative and severe reduction in permeability.

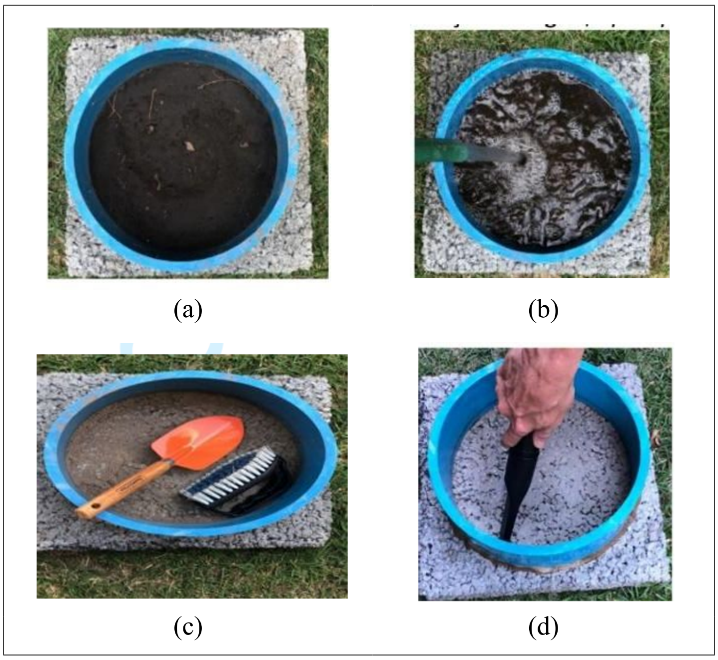

Figure 4 ▶ Simulation of clogging and maintenance of concrete slabs: a) material on the slab surface; b) water addition; c) removing the surface material and d) cleaning by suction and brushing. *Source: authors' archive*

Table 1 ▶ Particle size distribution of the clogging material. *Source: research data*

Sieve (mm)	12.7	9.5	4.8	2.4	1.2	0.6	0.31	0.15
Retained (%)	2.0	1.5	2.7	10.1	6.3	22.7	35.4	19.3

For the clogging process, an adaptation of the permeability test from ABNT NBR 16416 (ABNT, 2015) - Annex A was performed. In this adaptation, a 300 mm ring was fixed on the surface of each concrete slab to deposit the clogging material over a period of 7 days, while water flowed at a rate of 7.07 × 10^{-3} m³/day (Figure 4b) was adopted as a representative condition of urban surface runoff during low-to-moderate intensity rainfall events. This procedure was based on the methodology used by Sandoval *et al*. (2020), who also simulated the clogging process with water flow. A sediment mass of 3.2 kg was defined based on Tong (2011), who adopted similar values for simulated clogging processes in permeable pavements.

Maintenance of the permeable concrete slabs began with brushing and removing the surface material using a gardening brush and shovel (Figure 4c). After removing the surface material, vacuuming was performed with an NT-3.000 industrial vacuum cleaner (Figure 4d). The suction-based maintenance method was specifically selected due to the use of the geotextile membrane, which tends to reduce deep sediment penetration.

2.5 Simulation of peak flooding in a macro drainage system

For the modeling, the following areas: road system, sidewalks, medians, public squares, parks, and blocks within the A-6 sub-watershed were separated through an analysis of the basin's aerial photogrammetry, obtained in 2014. This separation of different areas was necessary due to the distinct permeability values found. Thus, a specific curve number (CN) was adopted for the area to accurately define effective precipitation based on the reference values determined for each soil and occupation following Tucci (2009). Table 2 presents the values of the areas.

Table 2 ► Percentage of areas within the A-6 sub-watershed. *Source: research data*

Area	Dimension (ha.)	%
A-6 watershed (marine slope)	816.16	100.00
Road system	114.47	14.02
Sidewalks	48.89	5.99
Medians	2.71	0.33
Public squares	8.28	1.03
Parks	20.75	2.54
Blocks	621.06	76.09

Rainfall data were obtained from station 363, administered by the Ceará Foundation for Meteorology and Water Resources (FUNCEME). The historical series available from 1974 to 2022 was considered. The maximum annual precipitation for this period was used for hydrological modeling. To estimate precipitation for return periods of 25, 50, and 100 years, the Log Pearson Type III distribution was used, which was validated through the Kolmogorov-Smirnov test at a 5% significance level ($\alpha = 0.05$). The values of the maximum daily precipitation are presented in Table 3.

Table 3 ► Maximum daily precipitation (mm) for different return periods. *Source: FUNCEME (2022)*

Return period (years)	**Maximum daily precipitation (mm)**
25	184.87
50	206.93
100	229.28

According to Torrico (1974), the municipality of Fortaleza-CE falls within Isozone C, which represents a maritime influence zone with mild rain coefficients. To determine the rainfall based on duration, intensity, and frequency, the rainfall data from FUNCEME station 363 were used, applying the coefficients proposed by Torrico (1974) for one hour and six minutes. The resulting discretized rainfall values are presented in Table 4.

Table 4 ▶ Discretized precipitation (mm) over time for different return periods. *Source: research data*

Return period (years)	Precipitation (mm)			
	1 day	24 hours	1 hour	6 minutes
25	184.87	203.36	79.72	19.93
50	206.93	227.62	88.32	22.31
100	229.28	252.21	96.85	22.19

For the modeling of peak flooding in the macro drainage system, a time of concentration (t) of 1.09 hours was adopted, corresponding to the duration of the design rainfall. The adopted concentration time was the one found by Bezerra (2007) for the basin analyzed by the kinematic method, due to the existing drainage system. Therefore, to determine the design precipitation (P), the Intensity Duration Frequency (IDF) equation was generated from the 24-hour and 1-hour rainfall data, as the estimated time of concentration falls within this duration interval.Table 5 presents the equations for return periods of 25, 50, and 100 years.

Table 5 ▶ IDF equation for different return periods. *Source: research data*

Return period (years)	Equation IDF
25	$P(t) = 38.904 \ln(t) + 79.72$
50	$P(t) = 43.832 \ln(t) + 88.32$
100	$P(t) = 48.885 \ln(t) + 96.85$

Thus, the design precipitation was estimated for a time of 1.09 hours. The effective precipitation was determined using the method proposed by SCS (1975), through the area curve numbers of the watershed. The rainfall simulation was performed for soil types "A," "B," "C," and "D" with their projections under both baseline (impervious) conditions and scenario projections incorporating permeable pavements. According to National Water Agency classification (ANA, 2018), Group A consists of soils with low runoff potential and high infiltration rates (minimum infiltration rate of 7 mm/h). Group B has a moderate infiltration rate with a minimum infiltration rate of 3.81 mm/h. Group C soils have a low infiltration rate, with a minimum infiltration rate of 1.27 mm/h. Group D represents soils with high runoff potential and very low infiltration rates (less than 1.27 mm/h). Table 6 presents the curve number values considered for the region in each scenario.

ISSN 2447-9187

Table 6 ▶
Curve number of urban components.
Source: research data

Soil region	Curve number							
	Waterproofed				Permeabilized			
	A	B	C	D	A	B	C	D
Road system	98	98	98	98	72	82	87	91
Sidewalks	98	98	98	98	72	82	87	91
Medians	98	98	98	98	72	82	87	91
Public squares	49	69	79	84	39	61	74	80
Parks	49	69	79	84	39	61	74	80
Blocks	77	85	90	92	77	85	90	92

2.6 Evaluation of locations for the application of permeable pavements in Fortaleza-CE

Based on the results of 300 georeferenced soil absorption index tests, a map of Fortaleza was generated, separating regions with soil types “A,” “B,” “C,” and “D,” according to the criteria adopted by ANA (2018). The determination of soil absorption was carried out during 2017 following the ABNT NBR 7229 (ABNT, 1993) standard. It was assumed that each test had an influence radius of 500 meters to ensure coverage of the map area. In locations where there was an overlap of the influence area, the soil with the higher surface runoff was given precedence. This allows for the compatibility of the different performances obtained in hydrological modeling for soil types “A,” “B,” “C,” and “D” with the application areas in Fortaleza. From this data, a mapping of the most favorable areas for the implementation of permeable pavements was generated.

3 Results and discussion

This section presents and discusses the main findings of the study, structured into three complementary analyses. First, the permeability performance of the concrete slabs is evaluated, considering the effects of clogging. Next, the hydrological modeling conducted for sub-basin A6 in Fortaleza is analyzed to assess the impact of permeable pavements on peak flow reduction under different scenarios. Finally, spatial mapping is used to identify priority locations for the application of permeable concrete pavements, providing a data-driven framework to support urban flood mitigation strategies.

3.1 Permeability analysis of concrete slabs

Tables 7 and 8 present the results of the infiltration tests, respectively, without and with the insertion of the geotextile, under the three conditions considered: (i) virgin (un-clogged) (ii) after the clogging process; (iii) cleaned (post-maintenance). For each slab and each scenario tested, two infiltration tests were performed and the average was considered. It should be noted that slabs 2, 4, and 5 were excluded from the analysis due to the occurrence of cement paste bleeding, which directly affects the permeability

ISSN 2447-9187

of the slabs. This effect can be attributed to the vibration and compaction process of the samples, which may have generated segregation of the concrete components. Bonicelli, Giustozzi and Crispino (2015) indicated that randomness in the compaction process, as well as the presence of excess fine material, can influence the permeability of porous concrete because it affects the quantity and distribution of voids. For the calculations of the mean (μ), standard deviation (σ), and Coefficient of Variation (CV), the values related to the slabs with bleeding were excluded.

Table 7 ►
Permeability (k) of concrete slabs without geotextile.
Source: research data

Batch	**Slab No.**	***k* (10^{-3} m/s) – Without geotextile**		
		(i – virgin)	**(ii – clogging)**	**(iii – clean)**
1	1	6.98	1.71	5.13
	2	–	–	–
	3	8.04	0.81	4.83
	μ	7.51	1.26	4.98
	σ	0.75	0.64	0.21
	CV (%)	9.99	50.79	4.26
2	7	7.97	0.61	2.57
	8	7.40	0.66	2.88
	9	7.07	0.81	2.88
	μ	7.48	0.69	2.78
	σ	0.46	0.10	0.18
	CV (%)	6.09	15.01	6.45

According to ABNT (2015), for a concrete pavement to be considered permeable, it must have a permeability greater than 1.00 $\times 10^{-3}$ m/s when newly constructed, a condition that all slabs evaluated in this study met. However, following the simulated clogging protocol, 9 slabs showed permeability lower than the recommended value. After the maintenance process, however, all slabs reached the normative minimum threshold, except for slab 5 of batch 1.

The variation in the permeability of the permeable concrete slabs may be associated with the randomness with which the compaction energy was applied during their molding process, with the aggregate rearranging due to the overlap of compaction energy (Bonicelli; Giustozzi; Crispino, 2015). Even when the drop height of the hammer and the number of blows is kept constant, this effect can be observed.

Table 8 ▶
Permeability of concrete slabs with geotextile.
Source: research data

Batch	Slab No.	k (10^{-3} m/s) – With geotextile		
		(i – virgin)	(ii – clogging)	(iii – clean)
1	4	–	–	–
	5	–	–	–
	6	7.10	0.53	3.61
	μ	–	–	–
	σ	–	–	–
	CV (%)	–	–	–
2	10	11.23	0.65	2.50
	11	11.54	2.34	2.15
	12	13.27	1.78	2.16
	μ	12.01	1.59	2.27
	σ	1.10	0.86	0.20
	CV (%)	9.15	54.14	8.78

The virgin slabs have lower dispersion. For all scenarios (with and without geotextile), permeability showed a CV below 10%. The clogged slabs exhibited greater dispersion, with CV values above 50% for slabs 1 and 3, and 15% for slabs 7, 8, and 9. After the maintenance process, the permeability values again showed a CV below 10% in all scenarios, indicating reduced dispersion. A possible explanation may be linked to the randomness throughout the clogging process, as there is no control over a preferred pathway for pore filling by the clogging material. As highlighted by Sandoval *et al*. (2022), accumulation of sediments (clogging) prevents the water flow to pass through the interconnected pores. However, the spatial distribution of the sediments is unpredictable, as it depends on size distribution of the clogging material as well as the size and distribution of the pores which influences permeability variation after clogging.

In the scenario with the insertion of the geotextile membrane, there is an average reduction in permeability under clogged condition, compared to the virgin slab, of 92.01%. After maintenance, the slabs showed an average permeability reduction of 75.82% compared to the virgin slabs. In the condition without the geotextile membrane, permeability decreases under the clogged condition by 87.49% compared to the virgin slabs, and in the post-maintenance situation, the slabs showed an average permeability reduction of 49.29% compared to the virgin condition. Thus, it is verified that the insertion of the geotextile membrane, for the case evaluated in this study, did not create benefits regarding the permeability of the slabs after clogging or after maintenance. It was expected that the presence of the geotextile one-third of the concrete slab, i.e., close to the surface, would facilitate the accumulation of sediments which could be sucked by the cleaning process. Consequently, it would be favorable to keep the permeability values always close to the original one (virgin concrete slab). However, this behavior was not observed. It is possible that part of the clogging material remained on the geotextile even after cleaning which affects the water flow.

It should be noted that when comparing the permeability of the concrete slabs with the hydrological classification of soils (ANA, 2018), the slabs without bleeding in their virgin condition and after maintenance displayed permeability consistent with type A soil, which is highly permeable and allows significant infiltration, typically composed of sandy soils that

ISSN 2447-9187

facilitate water absorption. In clogged conditions, slabs 1 and 12 matched the permeability of type B soil, which has moderate infiltration, generally a mix of sand and clay, allowing for some infiltration but also generating some surface runoff. The remaining slabs were similar to type C soil, which has low permeability and is often composed of clayey soils, leading to minimal infiltration and increased surface runoff. This analysis confirms that the permeable pavement, whether virgin or cleaned, is effective in reducing flood peaks for all foundation soil types and does not limit infiltration.

The results presented in Tables 7 and 8 highlight the influence of clogging and maintenance on the permeability of slabs with and without geotextile. While all virgin slabs met the minimum permeability required by ABNT (2015), a significant drop was observed after the clogging simulation. In slabs with geotextile, the permeability decreased by 92.01% under the clogged condition and remained 75.82% lower even after the cleaning process. In comparison, slabs without geotextile showed an average reduction of 87.49% after clogging and 49.29% after cleaning, relative to the virgin condition.

To better understand this hydraulic behavior, X-ray computed tomography was utilized to investigate the internal structure of the slabs. A total of six specimens were analyzed, comprising three slabs with geotextile and three slabs without geotextile. The porosity values reported correspond to the average of each group. As illustrated in Figure 5, slabs with geotextile (A and B) showed greater total volumetric porosity (48%, on average); however, the presence of the membrane appeared to disrupt the interconnection between pores, particularly in the upper third of the slab (Lima *et al*., 2024). This interruption may have hindered water flow through the structure, contributing to lower permeability even after the cleaning process. In contrast, slabs without geotextile (C and D) displayed a more continuous and interconnected porous network, with an average porosity of 15%, which explains the better recovery of permeability following maintenance (Lima *et al*., 2024). These microstructural observations reinforce that pore connectivity is more critical to permeability than porosity alone, as noted by Du Plessis *et al*. (2016).

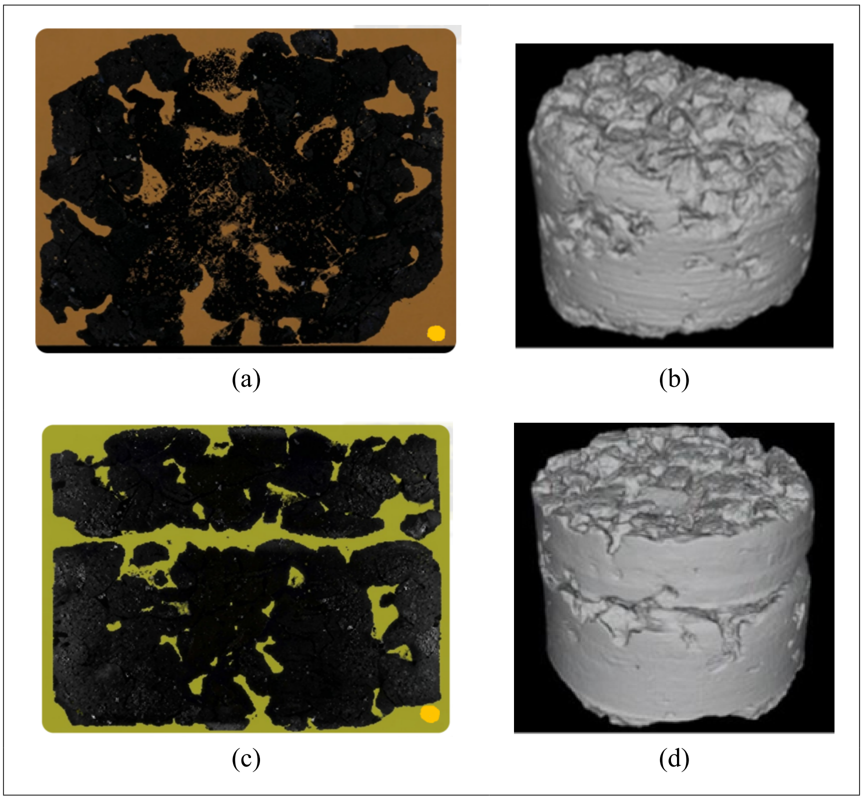

Figure 5 ▶ Tomographic analysis of PCP slabs with and without geotextile membrane: (a) Sagittal section and (b) 3D reconstruction of slab with geotextile membrane (PPCP-CG); (c) Sagittal section and (d) 3D reconstruction of slab without geotextile membrane (PPCP-SG). *Source: adapted from Lima et al. (2024)*

ISSN 2447-9187

The tomographic images provided evidence of this structural difference, supporting the hypothesis that the membrane insertion, while increasing total porosity, compromises the hydraulic efficiency of the slab by interrupting pore paths. Thus, tomography served as an essential tool to correlate microstructural characteristics with infiltration performance, especially under clogging and recovery conditions. The efficiency of water infiltration depends on the existence of a continuous "percolation backbone." According to Neithalath, Sumanasooriya and Deo (2010), even if a material exhibits high total porosity, its permeability can be significantly low if the pores are not well-interconnected. The lack of connectivity forces the fluid to follow a more winding and longer path, a phenomenon quantified as tortuosity. High tortuosity increases the internal resistance to flow and reduces the velocity of the water passing through the slab. Permeability is often limited by the size of the smallest openings between larger voids, known as pore throats. Sumanasooriya and Neithalath (2011) demonstrate that these "bottlenecks" control the overall flow rate. In the context of the present study, the insertion of a geotextile may create localized gaps at the interface increasing the total void volume recorded in tomographic scans but simultaneously obstruct these critical pore throats. This structural disruption interrupts the hydraulic paths, effectively clogging the material from the inside regardless of its total air content.

3.2 Hydrological modeling in sub-basin A6 in Fortaleza-CE

The curve number (CN) for type A soil was 80.28 in the baseline (impervious) and 74.63 in the permeable condition, showing a difference of 7.0%. For type B soil, the CN values were 87.08 in the impermeable condition and 83.54 in the permeable condition, with a difference of 4.0%. Type C soil had a CN of 91.24 in impermeable condition and 88.82 in the permeable condition, representing a difference of 2.6%. The values of 92.94 and 91.37 represent the CN for type D soil in the impermeable and permeable conditions, showing a difference of 1.7%. Therefore, the percentage reduction depends on the soil type, with a greater impact on type A soil, reaffirming the importance of soil type in the efficiency of implementing permeable pavements.

Nevertheless, it is noted that, regardless of the soil type, there is an improvement compared to the impermeable condition. Therefore, an analysis of each scenario where permeable pavements will be applied is necessary. Thus, Figures 6 and 7 present the peak flows for different soil types, for each return period, in both impermeable and permeable scenarios, respectively.

For a return period of 25 years, there is a reduction in peak flow between the impermeable and permeable conditions of 32%, 16%, 10%, and 6% for soil types A, B, C, and D, respectively. Evaluating the return period for 100 years, there is a decrease of 26%, 14%, 8%, and 5% in soil types A, B, C, and D, respectively. Thus, the influence of the soil type on which the permeable pavement will be implemented on its efficiency in reducing flood peaks is evident. The results found are consistent with the data presented by Drake, Bradford and Van Seters (2014), who found that increasing the fines content reduces the flood peak attenuation capacity.

Notably, the permeable pavement applied to soil type A has a performance four times higher than that installed on soil type D for all evaluated return periods. Soil type B showed, for all evaluated return periods, a percentage reduction in peak flow greater than 10%, while soil type C did not show a significant percentage reduction in peak flow for any return period.

ISSN 2447-9187

For a return period of 50 years, the peak flow in soil type A in an impermeable condition is lower than the peak flow for the same return period in soil types B, C, and D in a permeable condition. Soil type B, for the 50-year return period in an impermeable condition, presents a peak flow lower than that obtained for soil types C and D in a permeable condition for the same return period. Comparing, for the 50-year return period, soil type C in an impermeable scenario and soil type D in the permeable scenario, a percentage difference of 0.5% is found.

Furthermore, the peak flow for a 100-year return period in a permeable condition in soil type A is lower than the peak flow in a permeable condition for a 25-year return period in soils B, C, and D. For soil type B, with a 100-year return period, in a permeable condition, the peak flow is lower than the scenario of soil type D with a 25-year return period in a permeable condition. It is emphasized that the obtained results refer to the specifically analyzed basin; however, they allow for the observation of behavioral trends. Overall, the results indicate that soils with higher infiltration capacity (e.g., type A) significantly reduce peak flows even under extreme rainfall events, whereas soils with lower permeability (types C and D) show limited hydrological benefits, even with the implementation of permeable pavements. Consequently, this demonstrates that the effectiveness of permeable pavements is strongly dependent on subgrade soil characteristics, with greater flood mitigation potential in areas with favorable infiltration conditions. Additionally, the results highlight that, although permeable pavements contribute to peak flow attenuation, their performance may be insufficient to fully offset the impacts of urbanization in low-permeability soils under high return period events.

Figure 6 ▶
Peak flow (m^3/s) for each soil type at impermeable substrate.
Source: research data

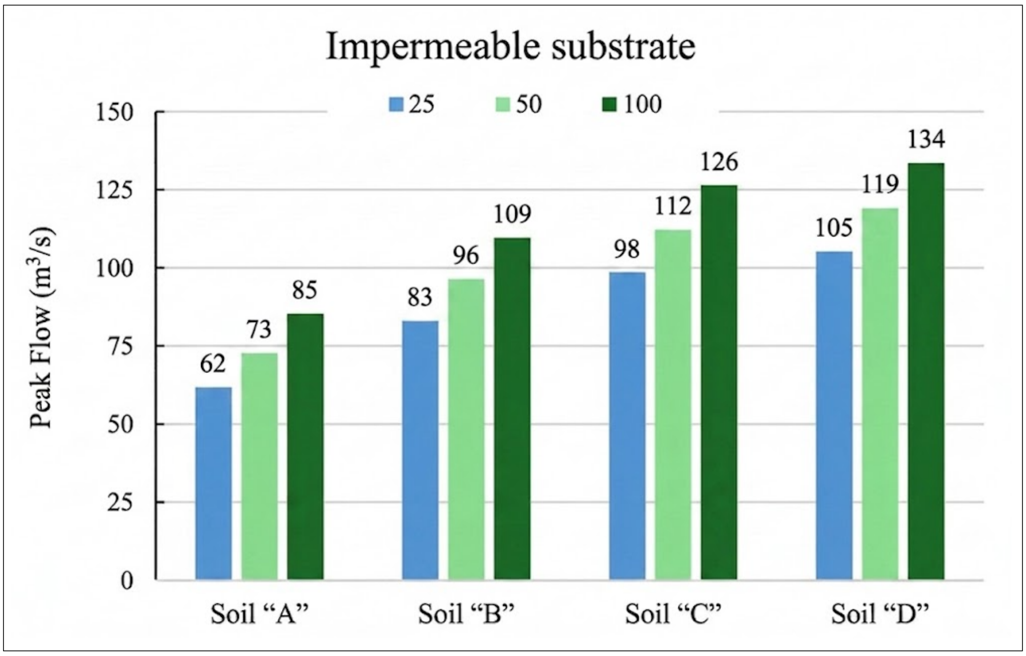

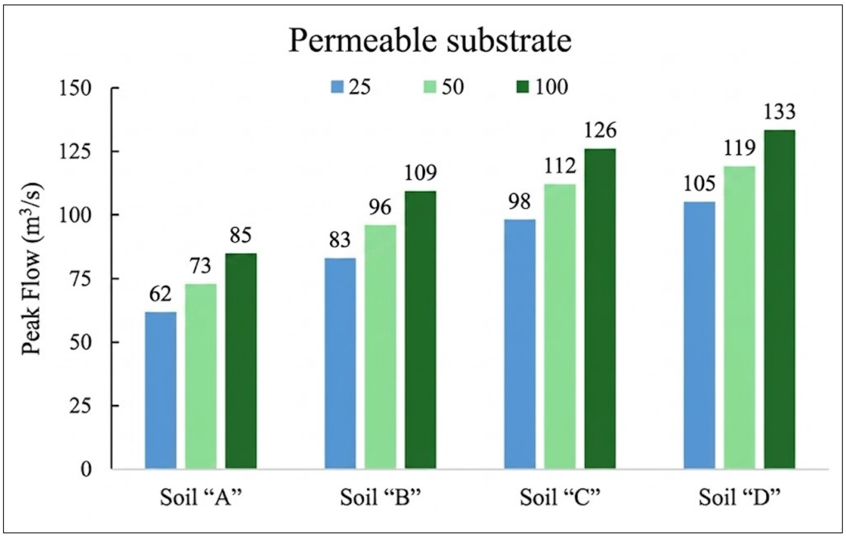

Figure 7 ► Peak flow (m³/s) for each soil type at permeable substrate. *Source: research data*

3.3 Mapping locations for the application of permeable concrete pavements in Fortaleza

From the analyses previously carried out, it was found that the type of subgrade soil in the region enhances the performance of permeable pavements when applied in locations where the soil promotes a greater infiltration process of rainwater. Thus, the A6 sub-basin analyzed in this research is in the maritime drainage basin, situated in the coastal region of Fortaleza, with sandy soil that presents a high infiltration rate. Figure 8 presents the map of Fortaleza constructed based on the 300 infiltration results and the respective soil classifications.

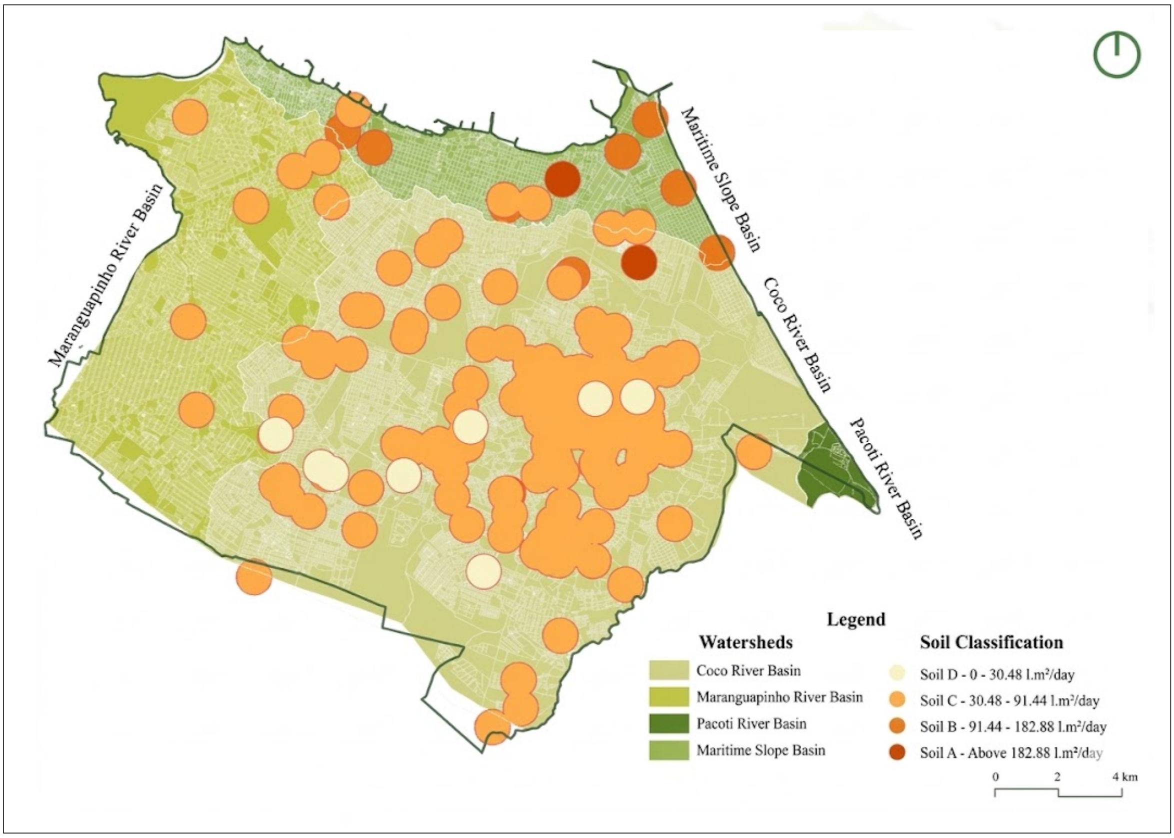

Figure 8 ▼ Map with soil type classification in Fortaleza for different river basins. *Source: prepared by the authors*

By analyzing Figure 8, soil C is the predominant type found in Fortaleza. However, in the coastal area, there is a higher concentration of type A and B soils. In contrast, as one moves away from the coastal area, there is an increase in the frequency of type D soil.

Thus, according to the data obtained from the surveys, the Maranguapinho River basin and the Cocó River basin predominantly contain type C soil. In the Cocó River basin, type A and B soils are also observed in the coastal region, and type D soil becomes more prevalent further inland, while in the Maranguapinho River basin, only type C soil was observed. The maritime drainage basin was the only one that predominantly presented soils with higher infiltration potential, such as type A and B soils. Therefore, this is the most suitable location for the application of permeable pavements in Fortaleza. It is important to note that this consideration cannot be generalized to the entire city, as there is lack of data obtained from the Pacoti River basin. Furthermore, urban planning and geotechnical constraints were not considered in this study and may influence the feasibility of implementation.

4 Conclusions

This study evaluated the influence of implementing permeable pavements under different conditions on the peak flow of an urban drainage system, advancing previous research by integrating experimental clogging analysis, permeability characterization, and hydrological modeling to assess how different subgrade soil types affect the effectiveness of permeable pavements in urban flood mitigation. The main contribution of this study is the integration of laboratory experiments, tomographic analysis, and hydrological modeling, enabling the correlation between pore-scale changes caused by clogging and their impacts on permeability and peak flow reduction at the urban drainage scale.

The results showed that the insertion of a geotextile membrane in the slabs did not improve the permeability rate under clogged conditions, not even after maintenance by suction. The slabs analyzed do not present a limitation for infiltration under the virgin condition and after maintenance, as they meet the minimum infiltration criteria. Regarding the clogging and cleaning process of the concrete slabs, further investigation is needed into the internal pore structure and the effectiveness of alternative cleaning strategies, such as high-pressure water jetting, mechanical sweeping, and combined vacuum-washing methods. In addition, although the tomographic analysis provided insights into pore distribution and connectivity, further studies are required to better understand the spatial distribution of clogging within the pore network, the depth of particle penetration, and the evolution of pore blockage over time.

It was found that the application of diffuse permeable pavements over a watershed can significantly reduce peak flows, and this effect is optimized when applied over more permeable soils. For the A6 sub-basin in Fortaleza, peak flow reductions of up to 20% were obtained with the application of permeable pavements. Due to the magnitude of the differences in flows with the change in soil type, it became evident that it is necessary to evaluate the locations where permeable pavements will be applied. In soils with low infiltration potential, the hydrological modeling results showed only limited reductions in peak flow compared to higher permeability soils, indicating that the effectiveness of permeable pavements for peak flow attenuation may be constrained under these conditions. However, it is important to note that permeable pavements can still provide additional benefits, such as reduction of total surface runoff volume, improvement of stormwater quality through filtration processes, and potential contribution to groundwater recharge.

Finally, the most suitable locations for the application of permeable pavements were found to be in the coastal region of the analyzed sub-basin, given the higher infiltration potential of the soil, and this result should not be generalized to the entire municipality of Fortaleza. However, every location has its peculiarities, making it necessary to refine the map generated for better accuracy by increasing the number of samples and developing new maps for other locations to more accurately select the preferential areas for the application of permeable pavements. It should be noted that the results obtained in this study refer to the analyzed basin, and it is recommended to evaluate peak flow reduction for other basins where permeable pavement can be implemented, considering the soil type and the available area for applying the investigated solution. Besides, for future studies it is suggested to evaluate the impact of lateral confinement on water flow in permeable concrete to maximize the effect of the porous pavement.

Funding

This research did not receive funding.

Conflict of interest

The authors declare no conflict of interest.

Note

This article originates from the master's thesis of the first author, Francisco de Assis Cavalcanti Bezerra, carried out at Federal University of Ceará in 2024, entitled "Avaliação do impacto no pico de cheia da implantação de pavimentos permeáveis sob diferentes condições como estratégia de drenagem urbana sustentável". Not available on the repository yet.

Authors' contribution

BEZERRA, F. A. C.: Conceptualization, methodology, investigation, formal analysis, writing – original draft. **LIMA, K.; RIBAS, L. V. S.:** Investigation, formal analysis, writing – review & editing. **FERREIRA, W. L. G.; CASTELO BRANCO, V. T. F.:** conceptualization, methodology, formal analysis, writing – review & editing, supervision. All authors participated in the writing, discussion, reading, and approval of the final version of the article.

References

ABNT – ASSOCIAÇÃO BRASILEIRA DE NORMAS TÉCNICAS. **ABNT NBR 7229**: Projeto, construção e operação de sistemas de tanques sépticos. Rio de Janeiro: ABNT, 1993. In Portuguese.

ABNT – ASSOCIAÇÃO BRASILEIRA DE NORMAS TÉCNICAS. **ABNT NBR 16416**: Pavimentos permeáveis de concreto – Requisitos e procedimentos. Rio de Janeiro: ABNT, 2015. In Portuguese.

AHIABLAME, L. M.; ENGEL, B. A.; CHAUBEY, I. Effectiveness of low impact development practices: literature review and suggestions for future research. **Water, Air, & Soil Pollution**, v. 223, p. 4253-4273, 2012. DOI: https://doi.org/10.1007/s11270-012-1189-2.

ANA – AGÊNCIA NACIONAL DE ÁGUAS. **Nota Técnica nº 46/2018/SPR**: Produção de base vetorial com o Curve Number (CN) para BHO 2014 (BHO_CN). Brasília, DF: ANA, 2018. Available at: https://metadados.snirh.gov.br/geonetwork/srv/api/records/d1c36d85-a9d5-4f6a-85f7-71c2dc801a67/attachments/NOTA_TECNICA_46_2018_SPR.pdf. Accessed on: 7 Oct. 2025. In Portuguese.

ASTM – AMERICAN SOCIETY FOR TESTING AND MATERIALS. **ASTM D6637**: standard test method for determining tensile properties of geogrids by the single or multi-rib tensile method. West Conshohocken: ASTM International, 2009.

BATEZINI, R.; BALBO, J. T.; HASELBACH, L.; CURVO, F. O.; KALLEDER, G. N.; SATO, B. S.; ZEMA, D. Experimental appraisal for characterizing laboratorial and field performance parameters of pervious concrete pavement. **Ambiente Construído**, v. 21, n. 2, p. 117-194, 2021. DOI: https://doi.org/10.1590/s1678-86212021000200520.

BEZERRA, F. A. C. **A problemática da drenagem de águas pluviais no município de Fortaleza-CE**: o caso da Bacia do Riacho Maceió-Papicu. 2007. Dissertação (Mestrado em Engenharia Civil) – Universidade Federal do Ceará, Fortaleza, 2007. In Portuguese.

BONICELLI, A.; GIUSTOZZI, F.; CRISPINO, M. Experimental study on the effects of fine sand addition on differentially compacted pervious concrete. **Construction and Building Materials**, v. 91, p. 102-110, 2015. DOI: https://doi.org/10.1016/j.conbuildmat.2015.05.012.

BROWN, R. A.; BORST, M. Evaluation of surface infiltration testing procedures in permeable pavement systems. **Journal of Environmental Engineering**, v. 140, n. 3, p. 1-12, 2014. DOI: https://doi.org/10.1061/(ASCE)EE.1943-7870.0000808.

DRAKE, J.; BRADFORD, A.; VAN SETERS, T. Hydrologic performance of three partial-infiltration permeable pavements in a cold climate over low permeability soil. **Journal of Hydrologic Engineering**, v. 19, n. 9, p. 1-9, 2014. DOI: https://doi.org/10.1061/(asce)he.1943-5584.0000943.

DU, S.; SHI, P.; VAN ROMPAEY, A.; WEN, J. Quantifying the impact of impervious surface location on flood peak discharge in urban areas. **Natural Hazards**, v. 76, p. 1457-1471, 2015. DOI: https://doi.org/10.1007/s11069-014-1463-2.

DU PLESSIS, A.; OLAWUYI, B. J.; BOSHOFF, W. P.; LE ROUX, S. G. Simple and fast porosity analysis of concrete using X-ray computed tomography. **Materials and Structures**, v. 49, p. 553-562, 2016. DOI: https://doi.org/10.1617/s11527-014-0519-9.

FUNCEME – FUNDAÇÃO CEARENSE DE METEOROLOGIA E RECURSOS HÍDRICOS. **Postos Pluviométricos**. 2022. Available at: http://www.funceme.br/?page_id=2694. Accessed on: 15 Apr. 2026. In Portuguese.

GARCIA, E. S. H. **Avaliação da progressão da colmatação de peças pré-moldadas de concreto permeável por meio de tomografia computadorizada**. 2022. Tese (Doutorado em Engenharia Civil) – Universidade Federal de Santa Catarina, Florianópolis, 2022. Available at: https://repositorio.ufsc.br/handle/123456789/247372. Accessed on: 6 Oct. 2025. In Portuguese.

HAWKINS, R. H.; THEURER, F. D.; REZAEIANZADEH, M. Understanding the basis of the curve number method for watershed models and TMDLs. **Journal of Hydrologic Engineering**, v. 24, n. 7, p. 1-8, 2019. DOI: https://doi.org/10.1061/(ASCE)HE.1943-5584.0001755.

KIA, A.; WONG, H. S.; CHEESEMAN, C. R. Clogging in permeable concrete: a review. **Journal of Environmental Management**, v. 193, p. 221-233, 2017. DOI: https://doi.org/10.1016/j.jenvman.2017.02.018.

LI, H.; KAYHANIAN, M.; HARVEY, J. T. Comparative field permeability measurement of permeable pavements using ASTM C1701 and NCAT permeameter methods. **Journal of Environmental Management**, v. 118, p. 144-152, 2013. DOI: https://doi.org/10.1016/j.jenvman.2013.01.016.

LIMA, K.; BEZERRA, F. A. C.; RIBAS, L. V. S.; FERREIRA, W. L. G.; BRANCO, V. T. F. C. Análise da relação entre a permeabilidade e a estrutura interna do concreto poroso. *In*: CONGRESSO DE PESQUISA E ENSINO EM TRANSPORTES (ANPET), 38., 2024, Florianópolis. **Anais** [...]. Florianópolis: ANPET, 2024. v. 3, 311234. Available at: https://proceedings.science/anpet/anpet-2024/trabalhos/analise-da-relacao-entre-a-permeabilidade-e-a-estrutura-interna-do-concreto-poro. Accessed on: 6 Oct. 2025. In Portuguese.

LIMA, M. S.; CHAVES, M. T. R.; AGUIAR, M. F. P.; FARIAS, T. R. L. Influência do resíduo de construção e demolição como agregado na produção de concreto para pavimentos permeáveis. **Revista Principia**, João Pessoa, v. 62, e8566, 2025. DOI: https://doi.org/10.18265/2447-9187a2024id8566. In Portuguese.

LIU, Z.; HE, C.; ZHANG, Q.; HUANG, Q.; YANG, Y. Extracting the dynamics of urban expansion in China using DMSP-OLS nighttime light data from 1992 to 2008. **Landscape and Urban Planning**, v. 106, n. 1, p. 62-72, 2012. DOI: https://doi.org/10.1016/j.landurbplan.2012.02.013.

LUCKE, T.; BEECHAM, S. Field investigation of clogging in a permeable pavement system. **Building Research & Information**, v. 39, n. 6, p. 603-615, 2011. DOI: https://doi.org/10.1080/09613218.2011.602182.

MARINHO, M. N.; COUTINHO, A. P.; SANTOS NETO, S. M.; CASAGRANDE, C. A.; SANTOS, G. T. L.; CARNEIRO, A. M. P. Mathematical modeling of the infiltration in a permeable pavement on the field scale. **Revista Brasileira de Recursos Hídricos (RBRH)**, v. 25, e39, 2020. DOI: https://doi.org/10.1590/2318-0331.252020200052.

MESQUITA, J. B. F.; PEREIRA, S. P.; LIMA NETO, I. E. Modelagem da drenagem urbana e avaliação das cargas bacteriológicas na Vertente Marítima de Fortaleza, Ceará. **Engenharia Sanitária e Ambiental**, v. 25, n. 1, p. 205-216, 2020. DOI: https://doi.org/10.1590/S1413-41522020189161. In Portuguese.

MIGUEL, B. H.; RENNÓ, C. D. Uso de dados de radar meteorológico em modelo hidrológico SCS-CN para a estimativa de escoamento superficial. **Revista Brasileira de Cartografia**, v. 72, n. 3, p. 501-516, 2020. DOI: https://doi.org/10.14393/rbcv72n3-53684. In Portuguese.

NEITHALATH, N.; SUMANASOORIYA, M. S.; DEO, O. Characterizing pore volume, sizes, and connectivity in pervious concretes for permeability prediction. **Materials Characterization**, v. 61, n. 8, p. 802-813, 2010. DOI: https://doi.org/10.1016/j.matchar.2010.05.004.

OLIVEIRA, L. C. B. **Análise da permeabilidade e da colmatação em concretos permeáveis produzidos com agregado reciclado de concreto**. 2017. Dissertação (Mestrado em Sistemas de Infraestrutura Urbana) – Pontifícia Universidade Católica de Campinas, Campinas, 2017. Available at: https://repositorio.sis.puc-campinas.edu.br/handle/123456789/1941. Accessed on: 6 Oct. 2025. In Portuguese.

RADFAR, A.; ROCKAWAY, T. D. Clogging prediction of permeable pavement. **Journal of Irrigation and Drainage Engineering**, v. 142, n. 4, p. 1-11, 2016. DOI: https://doi.org/10.1061/(ASCE)IR.1943-4774.0000975.

SANDOVAL, G. F. B.; GALOBARDES, I.; CAMPOS, A.; TORALLES, B. M. Assessing the phenomenon of clogging of pervious concrete (Pc): experimental test and model proposition. **Journal of Building Engineering**, v. 29, e101203, 2020. DOI: https://doi.org/10.1016/j.jobe.2020.101203.

SANDOVAL, G. F. B.; PIERALISI, R.; RISSON, K. D. B. S.; MOURA, A. C.; TORALLES, B. M. Clogging phenomenon in pervious concrete (PC): a systematic literature review. **Journal of Cleaner Production**, v. 365, 132579, 2022. DOI: https://doi.org/10.1016/j.jclepro.2022.132579.

SANSALONE, J.; KUANG, X.; YING, G.; RANIERI, V. Filtration and clogging of permeable pavement loaded by urban drainage. **Water Research**, v. 46, n. 20, p. 6763-6774, 2012. DOI: https://doi.org/10.1016/j.watres.2011.10.018.

SANSALONE, J.; TENG, Z. In situ partial exfiltration of rainfall runoff. I: quality and quantity attenuation. **Journal of Environmental Engineering**, v. 130, n. 9, p. 1008-1020, 2004. DOI: https://doi.org/10.1061/(ASCE)0733-9372(2004)130:9(990).

SARTORI, A. **Avaliação da classificação hidrológica do solo para a determinação do excesso de chuva do método do Serviço de Conservação do Solo dos Estados Unidos**. 2004. Dissertação (Mestrado em Engenharia Civil) – Universidade Estadual de Campinas, Campinas, 2004. Available at: https://repositorio.unicamp.br/acervo/detalhe/307232. Accessed on: 6 Oct. 2025. In Portuguese.

SCS – SOIL CONSERVATION SERVICE. **National Engineering Handbook**: Section 4 – Hydrology. Washington, D.C.: Soil Conservation Service, 1975.

SEIFEDDINE, K.; AMZIANE, S.; TOUSSAINT, E. State of the art on the hydraulic properties of pervious concrete. **Road Materials and Pavement Design**, v. 24, n. 11, p. 2561-2596, 2023. DOI: https://doi.org/10.1080/14680629.2022.2164332.

SUMANASOORIYA, M. S.; NEITHALATH, N. Pore structure features of pervious concretes proportioned for desired porosities and their performance prediction. **Cement and Concrete Composites**, v. 33, n. 8, p. 778-787, 2011. DOI: https://doi.org/10.1016/j.cemconcomp.2011.06.002.

TALEGHANI, M. Outdoor thermal comfort by different heat mitigation strategies: a review. **Renewable and Sustainable Energy Reviews**, v. 81, Part 2, p. 2011-2018, 2018. DOI: https://doi.org/10.1016/j.rser.2017.06.010.

TEIXEIRA, L. F. C.; MENESES FILHO, A. S. Avaliação de desempenho hidráulico de sarjetas no sistema de drenagem urbana: um estudo no bairro Aldeota, em Fortaleza (CE). **Revista Tecnologia**, v. 41, n. 1, p. 1-15, 2020. DOI: https://doi.org/10.5020/23180730.2020.10757.

TONG, B. **Clogging effects of Portland cement pervious concrete**. 2011. Master Thesis (Master's Degree in Civil Engineering) – Iowa State University, Amnes, 2011. DOI: http://dx.doi.org/10.31274/etd-180810-303.

TORRICO, J. J. T. **Práticas hidrológicas**. Rio de Janeiro: Transcon, 1974. 120 p. In Portuguese.

TUCCI, C. E. M. **Hidrologia**: ciência e aplicação. 4. ed. Porto Alegre: UFRGS: ABRH, 2009. In Portuguese.

VERMA, S.; SINGH, P. K.; MISHRA, S. K.; SINGH, V. P.; SINGH, S.; SINGH, A. Activation soil moisture accounting (ASMA) for runoff estimation using soil conservation service curve number (SCS-CN) method. **Journal of Hydrology**, v. 589, e125114, 2020. DOI: https://doi.org/10.1016/j.jhydrol.2020.125114.

WANG, J.; MENG, Q.; TAN, K.; ZHANG, L.; ZHANG, Y. Experimental investigation on the influence of evaporative cooling of permeable pavements on outdoor thermal environment. **Building and Environment**, v. 140, p. 184-193, 2018. DOI: https://doi.org/10.1016/j.buildenv.2018.05.033.

ZHOU, Y.; SMITH, S. J.; ZHAO, K.; IMHOFF, M.; THOMSON, A.; BOND-LAMBERTY, B.; ASRAR, G. R.; ZHANG, X.; HE, C.; ELVIDGE, C. D. A global map of urban extent from nightlights. **Environmental Research Letters**, v. 10, n. 5, e054011, 2015. DOI: http://doi.org/10.1088/1748-9326/10/5/054011.